

Chapter 3

Chiral-achiral lattice transitions

3.1 Introduction

In the last chapter we considered soliton states in nematics with a latent lattice order and showed that planar soliton states in the presence of an external field, can mediate transitions between two liquid crystalline phases -namely a chiral to an achiral phase. In this chapter, we consider other chiral-achiral phase transitions induced by external electric or magnetic fields or both. The transitions can take place through the formation of single soliton, disclinations and soliton lattices or even without the involvement of any defect.

In the previous chapter, we saw that a cholesteric (*Ch*) to nematic (N) transition takes place in a magnetic field H perpendicular to the axis of symmetry. This is an example of a soliton mediated transition. The transition is through the formation of a π soliton lattice whose period changes continuously with H , diverging at a critical field H_c . This transition is second order. Another example of a soliton lattice mediated transition is the transition from an S_C^* to S_C in a similar geometry under an external electric or magnetic field.

These transitions have been considered here in crossed electric and magnetic fields. As not much attention has been paid to these transitions in a field along the twist axis, we consider this geometry also.

In this chapter, field induced chiral-achiral transitions are discussed in cholesteric, ferrocholesteric (FC_h) and chiral Ferrosmeectics (FS_C) liquid crystals. We consider two geometries (i) Field along the symmetry axis and (ii) field perpendicular to the symmetry axis.

3.2 Transitions in a magnetic field along the axis of symmetry

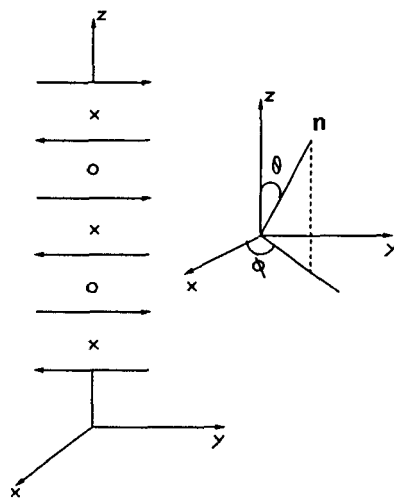


Figure 3.1: Schematic representation of an out of plane distortion in a cholesteric and the coordinate system used in describing the out of plane distortion

3.2.1 Cholesterics

The undistorted structure of a cholesteric in the absence of the field is given by $\mathbf{n}_0 = (\cos \phi_0, \sin \phi_0, 0)$ with $\phi_0 = 2\pi z/P$. In a field parallel to the twist axis the director \mathbf{n} will develop an out of plane distortion given by $n_x = \sin \theta \cos \phi$, $n_y = \sin \delta \sin \phi$ and $n_z = \cos \delta$. This is shown in Figure 3.1. The free energy density for this deformation in the one constant approximation is given by

$$F = \frac{K}{2} [(\nabla \theta)^2 + (\sin \theta)^2 (\phi_z^2 - 2q_0 \phi_z + f)] \quad (3.1)$$

This leads to the following equations of equilibrium

$$\nabla^2 \theta = \sin \theta \cos \theta [(\phi_z)^2 - 2q_0 \phi_z + f] \quad (3.2)$$

$$(\sin \theta)^2 \nabla^2 \phi = -2 \sin \delta \cos \theta [\nabla \theta \cdot (\phi_z - q_0) \hat{k}] \quad (3.3)$$

Here \hat{k} is the unit vector along the twist axis i.e., the z-axis. These two coupled equations permit the following solutions in ϕ and θ

$$\phi = q_0 z \quad (3.4)$$

$$\theta - \frac{\pi}{2} = 2 \tan^{-1} \left(\exp \left[\frac{z}{\eta_a} \right] \right) \quad (3.5)$$

where $\eta_a = \sqrt{1/(q_0^2 - f)}$. Equation (3.5) describes a planar soliton of width $2\eta_a$ with $\theta(-\infty) = \pi/2$ and $\theta(+\infty) = 3\pi/2$. Within this width the director goes out of the cholesteric plane and at the centre of the soliton the director is along the twist axis. The structure of this soliton is depicted in Figure 3.2.

We call this a 'Pinch Soliton' since the cholesteric lattice is pinched so to say in a narrow region of space. The width $2\eta_a$ of the pinch soliton, grows as the field increases and it diverges at a critical field given by $H_c = (2\pi/P) \sqrt{K/\chi_a}$. Hence we find a transition from the cholesteric state to the nematic state with

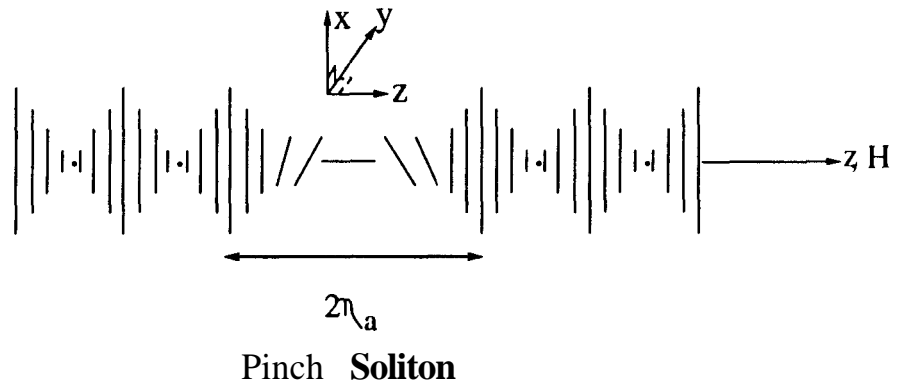


Figure 3.2: Structure of a longitudinal Pinch soliton. It has a δ variation along the twist axis.

the director \mathbf{n} everywhere along the twist axis of the parent cholesteric. It is important to mention here that the energy required to create such a pinch soliton gradually decreases and goes to zero as \mathbf{H} increases to H_C . Unlike the case of soliton lattice mediated transition, the period in the present geometry does not change with \mathbf{H} . We have a single soliton which grows in size and irons out the entire lattice at the critical field H_c . Interestingly this critical field is nearly $2/3$ of that obtained in soliton lattice mediated transition.

It is important to note that in this pinch soliton shown in Figure 3.2, ϕ and θ variations are in the same direction namely the twist axis. Hence we call this a longitudinal pinch. Equations (3.2) and (3.3) also permit a soliton solution with θ varying in a direction perpendicular to the twist axis. Here ϕ continues to vary along z . This transverse pinch soliton is shown in Figure

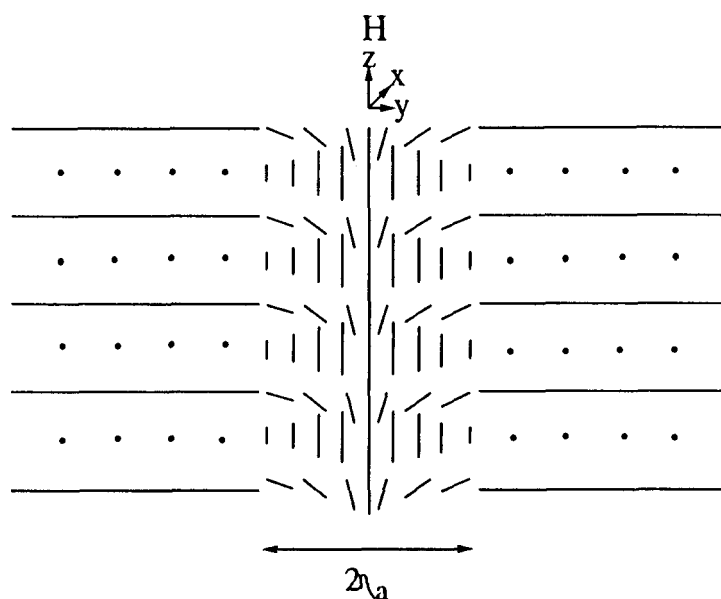


Figure 3.3: Structure of a transverse Pinch soliton with its θ variation perpendicular to the twist axis. It is a stack of twist and splay-rich solitons respectively.

3.3. As can be seen from the figure it is an alternate stack of twist and splay-rich solitons. The $Ch-N$ change can be brought about through the creation of either a longitudinal or a transverse pinch soliton. In this simple model we cannot assert as to which mode of transformation the system will adopt. However it is not difficult to see that in the presence of elastic anisotropy one of the pinch solitons will be of higher energy compared to the other. Therefore in a real system there will be no ambiguity. We have already discussed in the previous chapter that N to Ch transition can be brought about by a giant packet soliton. Hence in this geometry, both $Ch-N$ and $N-Ch$ transitions can be brought by a single giant soliton.

3.2.2 Ferrocholesterics

A ferrocholesteric (*FCh*) is obtained from an usual cholesteric by doping it with magnetic grains so that the local magnetization \mathbf{M} is along the local director \mathbf{n} i.e., \mathbf{M} spirals uniformly about the twist axis with a pitch \mathbf{P} . When unwound such a system would become a ferronematic (*FN*). The transition of an *FCh* to an *FN* in the presence of a magnetic field applied perpendicular to the twist axis has been considered by others [1], [2]. Here we consider the *FCh* – *FN* transition in a field applied parallel to the twist axis of an *FCh*.

Ferrocholesteric to ferronematic transition

The unperturbed state of the *FCh* is described by $\mathbf{n} = (\cos \phi_0, \sin \phi_0, 0)$ with $\phi_0 = 2\pi z/P$. The applied field is in the z direction. It results in an out of plane distortion in the director \mathbf{n} described by $n_x = \sin \theta \cos \phi$, $n_y = \sin \theta \sin \phi$ and $n_z = \cos \theta$. The free energy density is given by

$$F = \frac{K}{2} [(\theta_z)^2 + \sin^2 \theta (\phi_z^2 - 2q_0 \phi_z)] - \frac{\chi_a H^2}{2} \cos^2 \theta - MH \cos \theta \quad (3.6)$$

Minimization of the total energy yields

$$\theta_{zz} = \sin \theta \cos \theta [(\phi_z)^2 - 2q_0 \phi_z + f] + g \sin \theta \quad (3.7)$$

$$\sin^2 \theta \phi_{zz} = -2 \sin \theta \cos \theta [\theta_z (\phi_z - q_0)] \quad (3.8)$$

where $f = \chi_a H^2 / K$, $g = MH / K$, $\phi_{zz} = \partial^2 \phi / \partial z^2$ and $\theta_{zz} = \partial^2 \theta / \partial z^2$

The equations (3.7) and (3.8) permit the following solutions:

$$\phi = \phi_0 = q_0 z \quad (3.9)$$

$$\cos \theta = \frac{MH}{Kq_0^2 - \chi_a H^2} \quad (3.10)$$

It is clear from equations (3.9) and (3.10) that in the presence of the external magnetic field the pitch of the structure is unaltered and that θ is uniform throughout. When $0 < \theta < \pi/2$ we get a tilted $FC\mathbf{h}$. Since $\theta = 0$ in an FN we find that the transition from an $FC\mathbf{h}$ to an FN occurs at H_c with $MH_c = Kq_0^2 - \chi_a H_c^2$. The angle θ continuously decreases from $\pi/2$ as H increases from zero. Incidentally this transformation does not involve any defect.

Ferronematic to ferrocholesteric transition

Now we consider the FN obtained from the $FC\mathbf{h}$ in the manner described above. In this nematic state the director lies along the z direction. As we lower the field to $H < H_c$, we get θ and ϕ distortions described by $n_x = \sin \theta \cos \phi$, $n_y = \sin \theta \sin \phi$ and $n_z = \cos \theta$. In view of the degeneracy in θ with respect to the field direction, we set up the equations of equilibrium in cylindrical polars (r, α, z) . This leads to

$$\phi = q_0 z \pm N\alpha, N = \text{integer} \quad (3.11)$$

and the θ distortion obeys the differential equation

$$\theta_{rr} + \frac{1}{r}\theta_r = \frac{\sin \theta \cos \theta}{r^2} + (f - q_0^2) \sin \theta \cos \theta + g \sin \theta \quad (3.12)$$

Equations (3.11) and (3.12) permit a non-singular topological defect in n . At the centre of this defect θ is zero and far away from it θ is given by (3.10). The solution with $N = 1$ can be called a flower and it is rather similar to the all radial non-singular solution presented in chapter I, for a $\chi_a < 0$ nematic. The director at $r = \pm\infty$ is at a constant angle θ_0 with respect to the field and at the centre of the defect the director is along the field direction.

Through the formation of such topological defects we can enter the tilted FCh state. Given enough time, the unlike defects will attract and annihilate one another leading to an uniformly tilted FCh . Hence in this system one possible structural transformation, which is permitted by the equations of equilibrium, is that the achiral to chiral transition can be defect mediated while the chiral to achiral can take place without defects. However, in this transition, we can also have uniform θ solution without the formation of flowers provided there is a predisposition of the director to tilt in a particular direction due to sample boundaries.

Phase diagrams

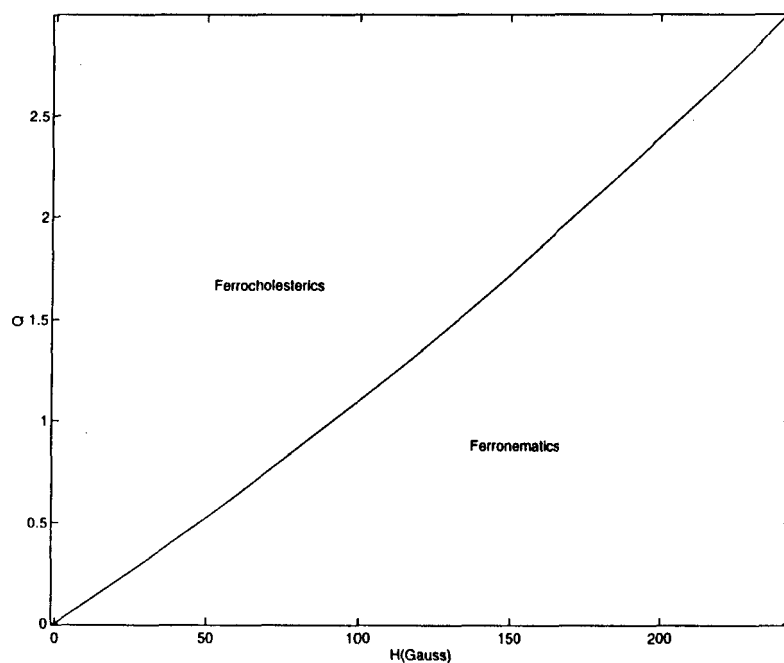


Figure 3.4: The transition from an FCh to an FN when $\chi_a > 0$. $Q = q_0^2$ in units of 10^{-5} cm^{-2} . $q_0 = 2\pi/P$ with P as the pitch of the FCh and H is the magnetic field. $M = 0.0001$ gauss and $\chi_a = 10^{-6}$ cgs units

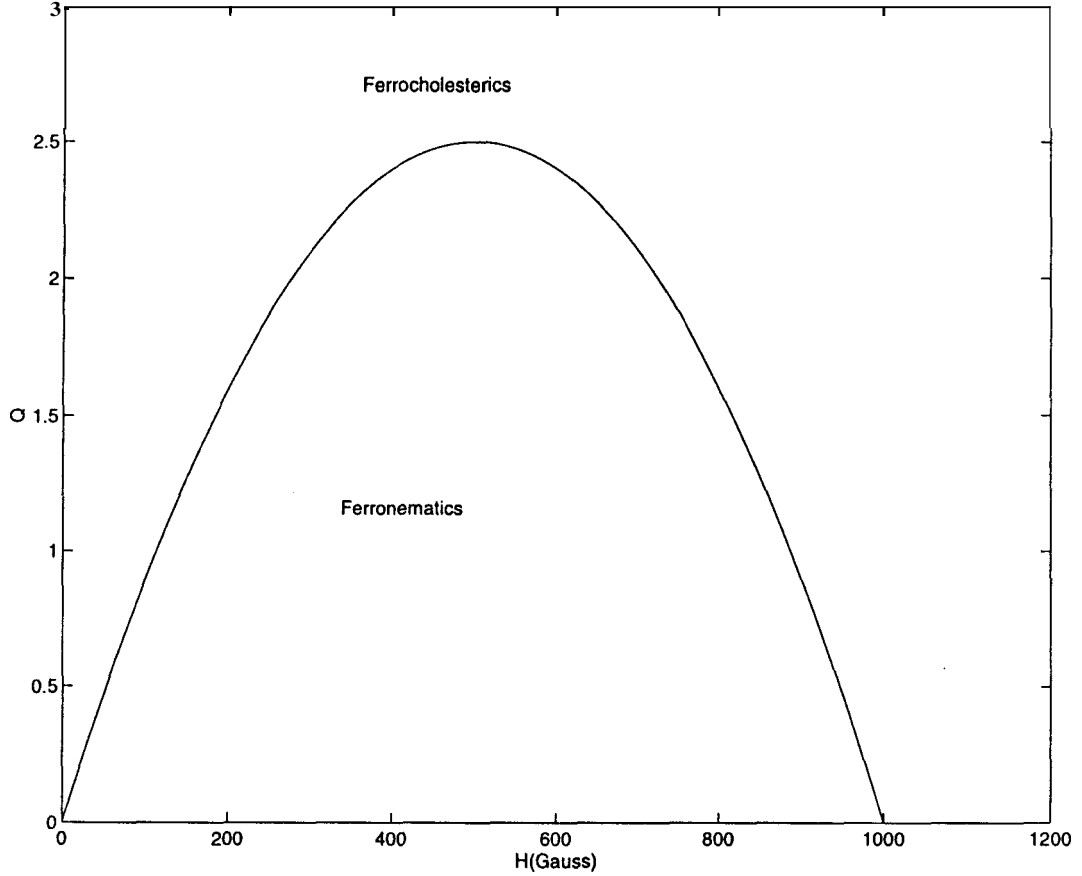


Figure 3.5: The transition from an *FCh* to an FN when $\chi_a < 0$. $\mathbf{M} = 0.0001$ Gauss and $\chi_a = -10^{-6}$ cgs units.

We showed that in *FCh*, on a gradual increase of the magnetic field, θ decreases monotonically and at a critical field H_c , *FCh* goes over to the FN state. The phase diagram for this transition is shown in Figure 3.4 for $\chi_a > 0$ systems. Here we have presented the phase diagram in the $H, Q(= q_0^2)$ space since it is possible to have cholesteric systems where q_0 can be varied continuously. This is possible both in compensated cholesterics [3] and in some pure systems [4]. We find a totally different phase diagram when $\chi_a < 0$. This is shown in Figure 3.5. We see that depending on the value of q_0^2 we get a

reentrance of FC_h on increase of the external field. For q_0^2 above a critical value the transition from FC_h to FN does not take place at all. This phase diagram can be easily understood from the fact that there are two opposing torques on the director, one due to the χ_a term which tilts the director towards the cholesteric planes and the other due to the M term which tilts it towards the twist axis. The net torque decides the state of the system. In view of the discussions presented in the previous section, we expect the FN to FC_h transition in this phase to be mediated by flower defects.

3.2.3 Ferrosmelectics

Ferrosmelectics(FS) are smectic systems which have been doped with magnetic grains. Such systems have already been made in lyotropic liquid crystals [5], [6]. We consider here an FS with the magnetic grains aligned such that the local magnetization M , is parallel to the local director n . We further make the system chiral by doping it with chiral molecules. It is possible for such a system to have in a magnetic field a low temperature chiral smectic C^* like phase (FS_{C^*}) and a high temperature achiral phase of smectic C (FS_C) or smectic A (FS_A) type. In our analysis of this system we take the electric polarization in the chiral phase to be negligible. We have considered the chiral-achiral transitions near the $FS_C(FS_A)$ - FS_{C^*} point. Generally, the tilt θ of n with respect to the layer normal can be assumed to be small.

Ferrosnematic C to ferrosmeectic A transition*

We first discuss the transition from FS_{C^*} to FS_A . The smectic layers of FS_{C^*} are in the $x-y$ plane with the director at an angle θ_0 with the layer normal. In the absence of the field the director configuration is $\mathbf{n}_0 \approx (\theta_0 \cos \phi_0, \theta_0 \sin \phi_0, 1)$ with $\phi_0 = 2\pi z/P$, P being the pitch of the helical structure. In the presence of a magnetic field H along z we find $n_x \approx \theta \cos \phi$, $n_y \approx \theta \sin \phi$ and $n_z \approx 1$. The free energy density is,

$$F = \frac{\alpha}{2}\theta^2 + \frac{\beta}{4}\theta^4 + \frac{K}{2}[(\nabla\theta)^2 + \theta^2(\phi_z^2 - 2q_0\phi_z)] + \frac{1}{2}\chi_a H^2 \theta^2 \pm \frac{MH\theta^2}{2} \quad (3.13)$$

The parameters α and β are the Landau coefficients. We consider the positive or the negative sign according as H is parallel or anti-parallel to \mathbf{M}_z , the component of \mathbf{M} along to the twist axis.

In the FS_{C^*} phase, $\theta \neq 0$ and α is negative equal to $-\alpha_0$. As in the case of ferrocholesterics here also in the chiral phase a uniform twist with a constant tilt are permitted solutions given by

$$\phi = \phi_0 = q_0 z \quad (3.14)$$

$$\theta = \sqrt{\frac{(\alpha_0 + Kq_0^2) - (\chi_a H^2 \pm MH)}{\beta}} \quad (3.15)$$

Transition from FS_{C^*} to FS_A occurs when

$$(\alpha_0 + Kq_0^2) - (\chi_a H^2 \pm MH) = 0 \quad (3.16)$$

This transition occurs by a continuous change in θ . In principle the critical fields for the transition are different for H parallel to \mathbf{M}_z and anti-parallel to

M_z cases. However with H anti-parallel to M_z and for $\chi_a < 0$ we do not get a transition to the FS_A state.

Ferrosmectic A to ferrosmectic C transition*

Consider an FS_A in a magnetic field parallel to the layer normal. In the absence of the field we have $\mathbf{n}_0 = (0, 0, 1)$. In this geometry if the magnetization \mathbf{M} is anti-parallel to H , we expect a tilt θ in the director \mathbf{n} with a ϕ degeneracy in the plane of the smectic layers. The director components are $\mathbf{n} = (\theta \cos \phi, \theta \sin \phi, 1)$. Since the phase is assumed to lack a mirror symmetry due to the presence of chiral molecules, this tilted director \mathbf{n} also precesses about the layer normal. In other words a tilt θ results in an azimuth ϕ which is a function of x , y and z . The free energy density for a $\chi_a > 0$ material is given by

$$F = \frac{\alpha}{2}\theta^2 + \frac{\beta}{4}\theta^4 + \frac{K}{2}[(\nabla\theta)^2 + \theta^2(\phi_z^2 - 2q_0\phi_z + (\phi_x^2 + \phi_y^2))] + \frac{1}{2}\chi_a H^2 \theta^2 - \frac{MH\theta^2}{2} \quad (3.17)$$

In the present case $a > 0$, as we are in the FS_A phase for which $\theta = 0$ when $H = 0$. Minimization of total energy leads to the following coupled equations.

$$\nabla^2\theta = \theta[a + (\phi_z)^2 - 2q_0\phi_z + (\phi_x^2 + \phi_y^2) + f - g] + b\theta^3 \quad (3.18)$$

$$S^2V^2g = -2\theta[\nabla\theta \cdot (\nabla\phi - q_0\hat{k})] \quad (3.19)$$

where $a = \alpha/K$, $b = \beta/K$ and k is a unit vector along z . Equations (3.18) and (3.19) permit the following solutions in cylindrical polars:

$$\phi = q_0z \pm N\alpha, \quad N = integer$$

And θ is assumed to be a function of r only. It obeys the differential equation

$$\theta_{rr} + \frac{1}{r}\theta_r = \theta\left[\left(a + \left(\frac{N}{r}\right)^2 + f\right) - (q_0^2 + g)\right] + b\theta^3 \quad (3.20)$$

The solution in ϕ describes a disclination of strength N with its associated ϕ pattern rotating as we go along the z axis. Equation (3.20) is the familiar *Ginsburg – Piteaviskii* equation. The tilt angle θ goes from zero at the centre of the disclination to a constant value θ_0 at a large distance from the centre [7]. Such field induced disclinations start interacting soon after creation. Given enough time unlike disclinations will annihilate one another resulting finally in an uniformly twisted FS_{C^*} phase with a tilt angle θ_0 . This θ_0 is given by

$$\theta_0 = \sqrt{\frac{(MN + Kq_0^2) - (\alpha + \chi_a H^2)}{\beta}} \quad (3.21)$$

It is clear from (3.21), that only for certain values of H we get a transition to the FS_{C^*} (i.e., $\theta_0 \neq 0$). This transition is second order. It is to be noted that, in the case of $\chi_a > 0$, for H parallel to M no phase transition to the FS_{C^*} takes place. And for $\chi_a < 0$, both with H parallel and anti-parallel to M we find that a transition to FS_{C^*} is possible at a critical field H_c . Interestingly, the critical fields in the two cases are different. Thus we see that the above analysis permits a disclination triggered transition from FS_A to FS_{C^*} and a defect free transition from FS_{C^*} to FS_A . Thus it is rather similar to $FCh - FN$ transition.

Phase diagram

- *Phenomenon of reentrance*

In the presence of the field, both in FS_A and FS_{C^*} , we get the phenomena

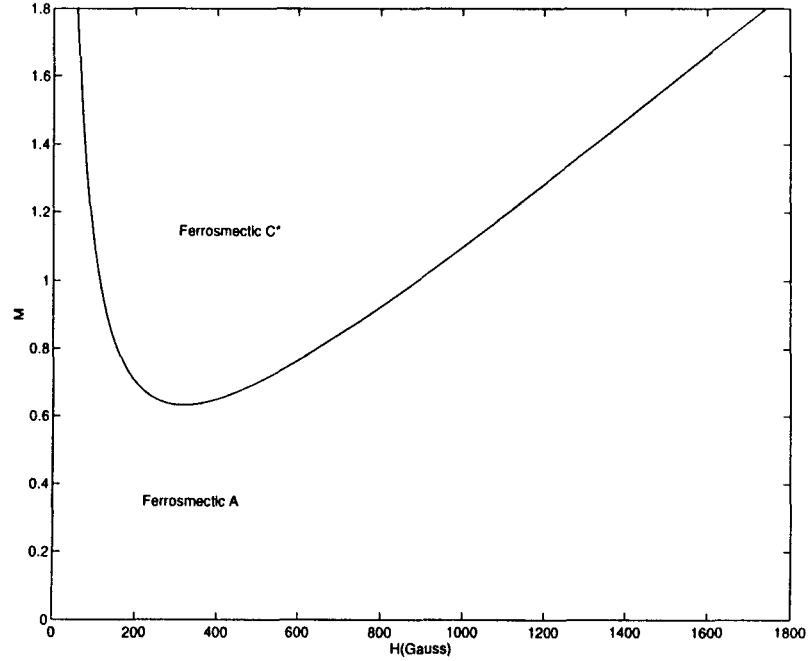


Figure 3.6: The phase diagram for the achiral FS_A phase. Here $\alpha = 1, \beta = 0.1, \chi_a = 0.1 * 10^{-6}$ and M_z and H are anti-parallel to one another. M is in units of 10^4 Gauss.

of reentrance. Figures 3.6 and 3.7 depict this. It should be noted that in both the cases the transition from the chiral to the achiral phase is not defect mediated while the transition from the achiral to the chiral phase is always through disclinations.

- *Tricritical point*

By incorporating higher order terms in the magnetic field contribution to the free energy, we can show that at a certain field the coefficient of the θ^4 term can change sign. Beyond this field, the $FS_A - FS_{C^*}$ phase boundary becomes first order. Therefore we can expect a tricritical point on this phase boundary. At this point a second order phase transition

goes over to a first order phase transition. Hence this phase change at high fields can become first order above a certain value of H while at low fields it is second order.

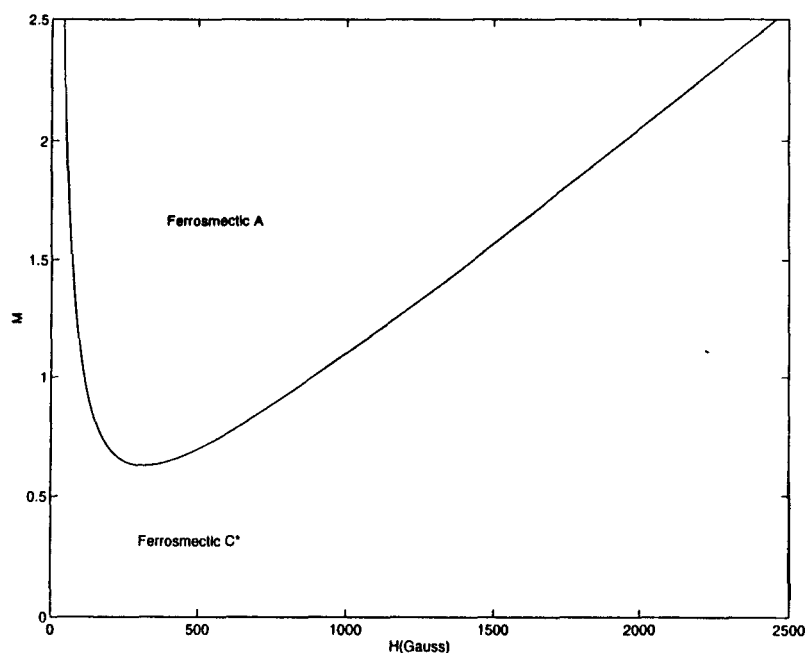


Figure 3.7: The phase diagram for the chiral FS_{C^*} phase. Here $\alpha_0 = -0.02$, $\chi_a = -0.1 \times 10^{-6}$, $\beta = 0.1$ and M_z and H parallel to one another. M is in units of 10^4 Gauss.

Grain migration

It is well known that in a magnetic field acting perpendicular to the twist axis of an FCh the magnetic grains migrate out of highly distorted regions to regions of low distortion. The same phenomenon can be expected in FS_{C^*} also in the same geometry. We have seen that in both FCh and FS_{C^*} in a magnetic field parallel to the twist axis the ϕ and θ distortions are uniform all over. Hence in this geometry we find FCh to FN or FS_{C^*} to FS_A transition to take place without grain migration. Even when we go from FN to FCh or FS_A

to FS_{C^*} though non-uniform distortions result due to the creation of defects, these get ironed out quickly due to the attraction between unlike defects. Therefore even here, there will be no grain migration. This is the unusual feature of these chiral-achiral transitions in ferrosystems in this geometry.

3.2.4 Remarks

It may be mentioned that all the structural transitions discussed so far are permitted solutions to the equations of equilibrium. The solutions are such that a uniform twist exists in the medium even in the presence of an external field. However, there could be other solutions with a non-uniform twist and a different θ variation. These may even have lower energies. Hence the structural transition suggested here, in any particular case should be looked upon as one of the possible modes of transition from a twisted configuration of the director field to the untwisted one and vice versa.

3.3 Transitions in crossed electric and magnetic fields

So far we considered transformations in a magnetic field acting along the symmetry axis. The process of chiral – achiral transition will be very different in a field perpendicular to the symmetry axis, This has already been discussed in literature for cholesterics [8] [9] ferrocholesterics [1, 2] and S_{C^*} [10, 11]. In the case of S_{C^*} , the transitions have been considered in the neighbourhood of $S_A - S_{C^*}$ point. These transitions are mediated by the creation of soliton lattices which at a critical field go over to the achiral phase. Here we consider

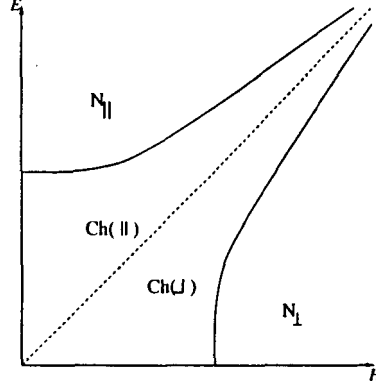


Figure 3.8: *The schematic phase diagram for a cholesteric in crossed fields. N_{\parallel} and N_{\perp} denote nematics which are aligned parallel and perpendicular to the H field respectively. $Ch(\parallel)$ denotes a cholesteric soliton lattice with nematic regions aligned parallel to the field and $Ch(\perp)$ denotes that which has the nematic regions aligned perpendicular to the field.*

the same phase transitions but in crossed electric (E) and magnetic (H) fields.

3.3.1 E and H perpendicular to the twist axis

We consider transitions in Ch and FCh systems in crossed electric and magnetic fields both in a plane perpendicular to the symmetry axis *viz.*, the twist axis.

Cholesterics

Consider a cholesteric with a magnetic field H along the x axis and an electric field E perpendicular to it along the y axis. The director configuration is described by $\mathbf{n} = (\cos \phi, \sin \phi, 0)$. The free energy density is given by

$$F = \frac{K}{2} [(\phi_z^2 - 2\phi_z q_0)] - \frac{\chi_a}{2} H^2 \cos^2 \phi - \frac{\hat{\epsilon}_a}{2} E^2 \sin^2 \phi \quad (3.22)$$

where $\hat{\epsilon}_a = \epsilon_a / (4\pi)$ with ϵ_a as the dielectric anisotropy. We consider the case

of $\chi_a > 0$ and $\epsilon_a > 0$ systems. Minimization of the total energy gives

$$\phi_{zz} = \frac{(\chi_a H^2 - \hat{\epsilon}_a E^2)}{K} \sin \phi \cos \phi \quad (3.23)$$

This is similar to the equation found in cholesterics. Hence the transition is driven by the formation of a π soliton lattice which on increase of either electric or magnetic field goes over to a nematic state aligned along the magnetic field ($N_{||}$) or to a nematic state aligned perpendicular to the magnetic field (N_{\perp}) depending upon whether $\chi_a H^2$ is more or less than $\hat{\epsilon}_a E^2$. The phase diagram is schematically shown in Figure 3.8. Here $Ch(||)$ represents a soliton lattice where the nematic regions are parallel to the magnetic field and $Ch(\perp)$ represents the one where the nematic regions are perpendicular to the magnetic field. As can be seen from Figure 3.8, a continuous change of E (or H) above a threshold H (or E) results in a change of the nematic phase from the $N_{||}$ to the N_{\perp} state or vice versa through the formation of a cholesteric structure is possible. The cholesteric-nematic phase boundaries are given by

$$\pm (\chi_a H^2 - \hat{\epsilon}_a E^2) = \frac{K q_0^2 \pi^2}{4} \quad (3.24)$$

Ferrocholesterics

We consider a ferrocholesterics (FCh) in the same geometry of crossed fields. Here we have to solve numerically two coupled differential equations one for ϕ distortions and another for grain migration. A very similar problem has already been considered [2]. We summarize here its implications since its generalization to the present problem is trivial.

We find that FCh to FN transition takes place as shown schematically in Figure 3.9 for $\chi_a > 0$ and $\epsilon_a > 0$. The FCh goes to the FN state either

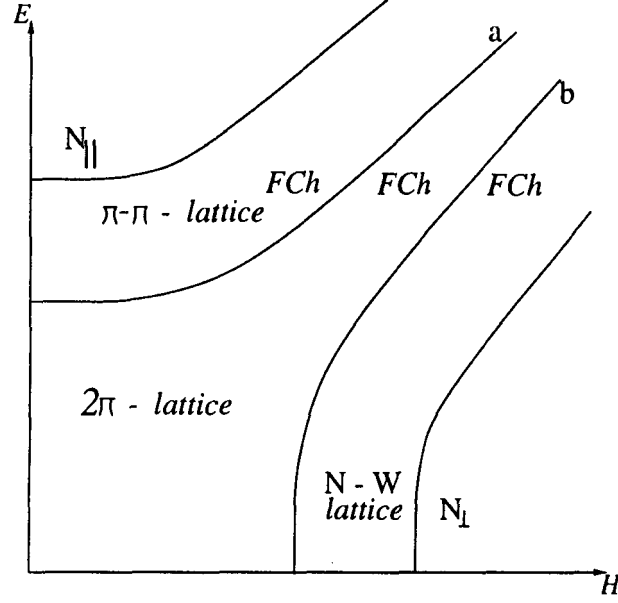


Figure 3.9: Schematic phase diagram for an *FCh* in crossed fields. Here *a* denotes the phase boundary $MH = \chi_a H^2 - \epsilon_a E^2$ and *b* denotes $MH = \epsilon_a E^2 - \chi_a H^2$.

through the sequence of a 2π soliton lattice followed by a split 2s i.e., $\pi - \pi$ soliton lattice and ultimately to a N_{\parallel} ferronematic or through the sequence of a 2π lattice followed by an N – W soliton lattice and finally to a N_{\perp} ferronematic state. In the $\pi - \pi$ soliton lattice, the repeat unit is a pair of π -solitons. However, in the N – W soliton each repeat unit is again a pair of solitons but of type N and type W which respectively have twists from $-\theta_0$ to θ and θ to $2\pi - \theta_0$ with $\theta_0 = \cos^{-1}(M/\chi_a H)$. The transformation of the 2π lattice to either $\pi - \pi$ lattice or N – W lattice takes place along the phase boundaries

$$MH = \pm(\chi_a H^2 - \epsilon_a E^2) \quad (3.25)$$

These lattices on further increase of the field go over to N_{\parallel} or N_{\perp} ferronematics. This phase boundary can only be numerically evaluated. It may be mentioned that for $\chi_{\mathbf{a}} < 0$ and $\epsilon_{\mathbf{a}} < 0$ ferrocholesterics, the regions of $\pi - \pi$ lattice and $N - W$ lattice get interchanged in the phase diagram. In all these soliton mediated $FCh - FN$ transition, we will have migration of magnetic grains. Interestingly, the grain profiles for $\pi - \pi$ and $N - W$ soliton lattices are entirely different [2]. Even here, through a continuous change of E (or H) above a threshold H (or E) a change of the nematic state from N_{\parallel} to N_{\perp} and vice versa via FCh is possible. In a similar way we can also discuss the case of $\chi_{\mathbf{a}}$ and $\epsilon_{\mathbf{a}}$ being of opposite signs.

3.3.2 H along and E perpendicular to the symmetry axis

We now consider field induced chiral – achiral transformations in ferrochiral smectic (FS_{C^*}) with H along and E perpendicular to the symmetry axis i.e., $H = (0, 0, H)$, $E = (E, 0, 0)$ and $\mathbf{n} = (0 \cos \phi, \theta \sin \phi, 1)$. Here again we assume δ to be small and grain migration to be negligible. The free energy density without grain migration is

$$F = \frac{\alpha}{2}\theta^2 + \frac{1}{4}\beta\theta^4 + \frac{K}{2}[(\theta_z)^2 + \theta^2((\phi_z)^2 - 2q_0\phi_z)] \quad (3.26)$$

$$+ \frac{1}{2}\chi_{\mathbf{a}}H^2\theta^2 - \frac{1}{8\pi}\epsilon_{\mathbf{a}}E^2\theta^2(\cos \phi)^2 \pm \frac{MH}{2}\theta^2$$

Thermal phase transitions in chiral smectic (S_{C^*}) due to a rather similar free energy density has been worked out by Michelson [12] and Yamashita [10, 11] but in a E or H perpendicular to the twist axis. We state here their main results. Michelson theoretically suggested the possibility of a Lifshitz

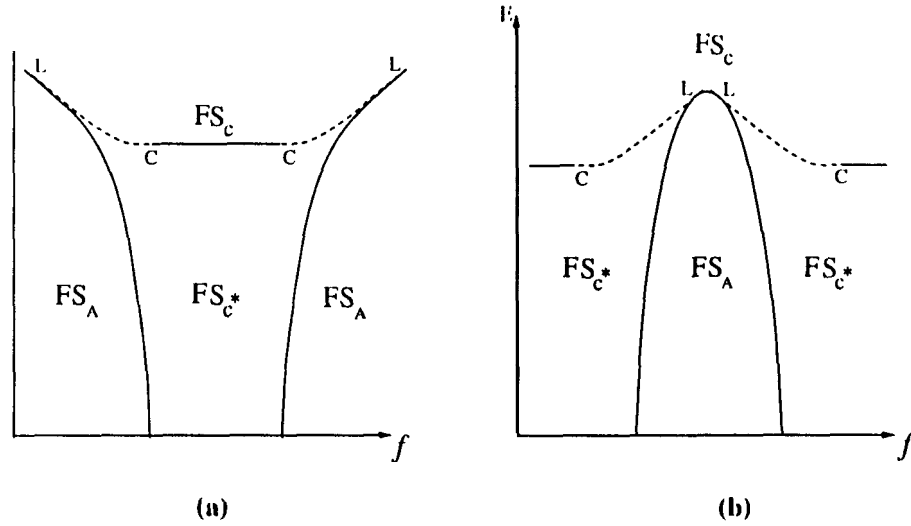


Figure 3.10: A possible schematic phase diagram of a $\epsilon_a > 0$ ferrosmeectic in crossed fields. For (a) $a > 0, \chi_a > 0$ and $M \cdot H \neq 0$. (b) $a < 0, \chi_a < 0$ and $M \cdot H \neq 0$. The full line represents second order phase transition and the dashed line the first order transition. Points C and L represent tricritical and Lifshitz point respectively. Here $f = (\chi_a H^2 + MH)$

point in the vicinity of $S_C - S_{C^*} - S_A$ transition point. A Lifshitz point is a modified triple point at which disordered, completely ordered and modulated phases meet. He predicted the phase diagrams for both $\chi_a > 0$ and $\chi_a < 0$ materials. He also conjectured that the S_C to S_{C^*} transition must be first order. Yamashita undertook a detailed study on the existence of various kinds of soliton mediated transitions between S_{C^*} and S_C phases in a similar geometry. He also, like Michelson concluded that in the presence of a magnetic field the S_C to S_{C^*} phase transition need not be a second order transition.

We can easily extend their results to ferrochiral smectics in a configuration where H is along and E is perpendicular to the twist axis with the system at a constant temperature. We find that this system has phase diagrams which are

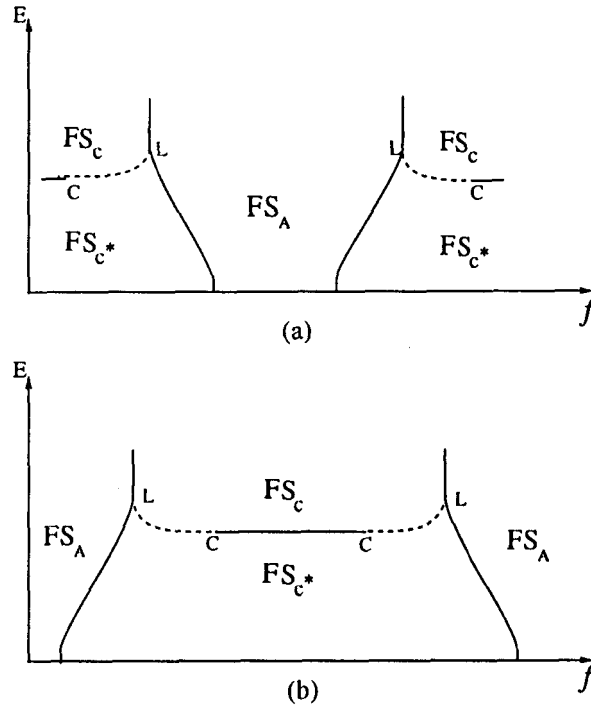


Figure 3.11: A possible schematic phase diagram for $\epsilon_a < 0$ ferrosmectic in crossed field. The notations are the same as those of Figure 11. For (a) $M \cdot H > 0$, $\alpha < 0$, $\chi_a < 0$ and for (b) $M \cdot H < 0$, $\alpha > 0$ and $\chi_a > 0$. Here $f = (\chi_a H^2 + MH)$.

interesting variations of those obtained by Michelson and those of Yamashita. Two of the very interesting possible phase diagrams are shown schematically in Figures 3.10 and 3.11. These are respectively for $\epsilon_a > 0$ and $\epsilon_a < 0$ materials. We find that this system can exhibit the features of reentrance together with tricritical point C and Lifshitz point L . The essential features of this phase diagram can be easily understood. For $(\alpha + \chi_a H^2 + MH) \ll 0$ we can expect what Yamashita and Michelson predict in the low temperature region of S_C i.e., a second order FS_{C^*} to FS_C transition. In the neighbourhood of $(\alpha +$

$\chi_a H^2 + MH) = 0$, this transition becomes first order resulting in a tricritical point C on the $FS_{C^*} - FS_C$ phase boundary. For $(\alpha + \chi_a H^2 + MH) \gg 0$ this phase boundary meets the $FS_C - FS_A$ phase line tangentially at the Lifshitz point L . These arguments hold good for both $\epsilon_a > 0$ and $\epsilon_a < 0$ case as well.

3.3.3 Remarks

We have intentionally not considered the following geometries in our study.

- i) FS_{C^*} and FCh with E along the twist axis and H perpendicular to it.
- ii) FS_{C^*} with E and H perpendicular to the twist axis.
- iii) Cholesterics with E (or H) parallel to the twist axis and H (or E) perpendicular to the twist axis.

We make the following comments regarding these geometries. In geometry (i) due to the $M \cdot H$ term in the free energy density the FS_A phase will not exist. Also if $\chi_a = 0$, we can expect a phase diagram similar to that obtained by Yamashita [13] for a ferroelectric S_{C^*} with $\epsilon_a = 0$ and in an electric field parallel to the smectic planes. There will be no FS_A phase and the FS_{C^*} to FS_C phase boundary will have two tricritical points. This is shown in Figure 3.12. However when $\chi_a \neq 0$ we can extrapolate the results of magnetic field effects on an FCh and electric field effects on a ferroelectric S_{C^*} . It has been shown that in the case of FCh , in a magnetic field perpendicular to the twist axis, to start with we get a 2π soliton lattice which transforms to either a $\pi - \pi$ soliton lattice ($\chi_a > 0$) or a $N - W$ soliton lattice ($\chi_a < 0$) at a certain field H . A very similar result can be expected in the case of FS_{C^*} also. This phase transition is second order. Therefore we expect a new phase

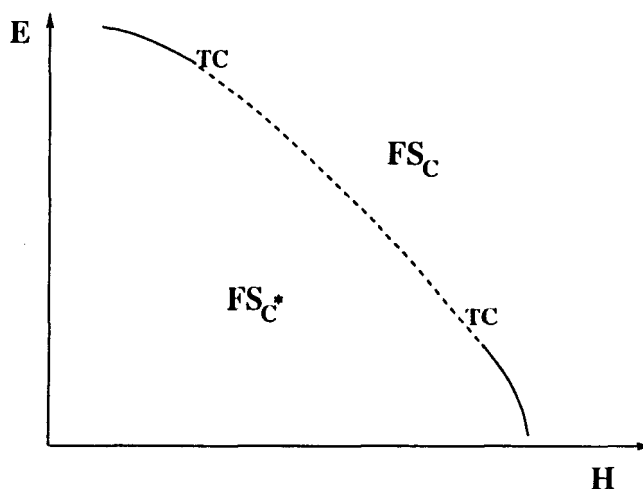


Figure 3.12: Schematic representation of FS_{C^*} - FS_C phase boundary showing TC as the tricritical point.

boundary in the FS_{C^*} region before it goes over to FS_C . This phase boundary corresponds to a transition from a 2π soliton lattice to a $\pi - \pi$ or N - W soliton lattice. At low magnetic fields (acting along the twist axis) we can expect this transition to be still second order. However at high magnetic fields it will be different in view of the fact that the soliton structure is quite unusual in this region. Here even a single 2π soliton has ripples in its ρ profile. Extending the arguments of Yamashita we speculate that this leads to an attraction between like 2π solitons resulting in a first order transition from the 2π soliton lattice to a $\pi - \pi$ or N - W soliton lattice. Therefore we expect on this new phase boundary a tricritical point as well. The way this new phase boundary meets

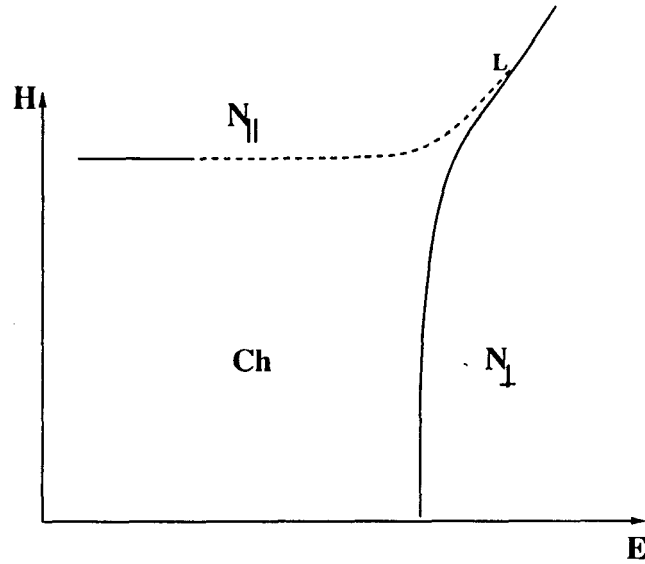


Figure 3.13: Schematic representation of $Ch - N$ transition with crossed fields.

the $FS_C - FS_C$ boundary is not easy to speculate upon. All these features are plausible even in the case of an FCh in a similar geometry. In geometry (ii) the phase transition is qualitatively similar to an FCh in the same geometry. We conjecture that in geometry (iii), we can expect a phase diagram similar to that obtained by Yamashita [II] for ferroelectric S_C in a magnetic field along the layers. Here we will be having a phase transition from Ch to $N_{||}$ and Ch to N_{\perp} states in the place of FS_C and FS_A states. This phase diagram is shown in Figure 3.13.

It should be emphasized that phase diagrams in all these cases can be constructed only by undertaking detailed and elaborate calculations pertaining

to the structure and energetics of the soliton lattices.

3.4 Effect of boundaries

It has been implicitly assumed in the case of $FC\mathbf{h} - FN$ and $Ch - N$ transitions, that a global reorientation of the helical axis perpendicular to the field is prevented by sample boundaries. In the case of FS with \mathbf{M} anti-parallel to \mathbf{H} , a global flip of the sample to the configuration of \mathbf{M} parallel to \mathbf{H} is again assumed to be prevented by the sample boundaries. In this context a few remarks on the boundary effects are in order.

In Ch and $FC\mathbf{h}$ systems we can easily realise in the laboratory two boundary conditions viz., the twist axis is either parallel or perpendicular to the bounding surface. These are shown in Figure 3.14. In FS systems likewise, we have two boundary conditions viz., smectic layers are either parallel or perpendicular to the bounding surface. In such situations our values of θ and ϕ should be matched smoothly with the values of θ and ϕ existing at the boundaries of the sample. This takes place over a coherence length in the neighbourhood of the sample boundaries. The value of the coherence length depends upon the field and elastic constants. Though this can be explicitly included in each problem we may still expect many of our solutions to be reasonably valid in large enough samples under appropriate boundary conditions. In particular, we make the following observations:

- (1) In the case of FS we can easily orient the layers but cannot anchor θ or ϕ at the boundaries. Hence for both the boundary conditions solutions discussed for this case will be valid.

-
- (3) In all the situations in section 3.2, where the field induces a soliton lattice the appropriate boundary condition to be chosen is that where the twist axis is perpendicular to the wall or where the smectic layers are parallel to the walls. Then all the solutions discussed under this section are valid.
- (4) In all the other cases, the solutions obtained can be matched with either of the boundary conditions viz., the twist axis is parallel or perpendicular to the walls. This matching can be effected over a coherence length near the bounding surfaces. Further, for FN to FC_h transition, for both boundary conditions, the director is already predisposed to tilt in a particular direction. Hence this transition will not be defect mediated.

Bibliography

- [1] Brochard F. and de Gennes P.G., *J. Physique* **31** (1970) 691
- [2] SunilKumar P.B. and Ranganath G.S. , *J. Physique* **3** (1993) 1497
- [3] Friedal G. *Ann. Phys* **18** (1922) 273. See also Ranganath G.S., Suresh K.A., Rajagopalan S.R and Kini U.D *Pramana, Suppl* (1975) 353
- [4] Dierking I., Giebelmann F., Zugenmaier P., Mohr K., Zschke H. and Kuczynski W., *Liquid Crystals* **18** (1995) 443
- [5] Ponsinet V., Fabre P., Veysie M. and Cabanel R., *J. Phys II* **4** (1994) 1785
- [6] Ponsinet V., Fabre P. and Veysie M. , *Europhys. Lett.* **30** (1995) 277
- [7] Ranganath G.S. , *Mol. Cryst. Liq. Cryst. Lett.* **92** (1983) 201
- [8] deGennes P.G., *Sol. State Commun.*, **6** 163 (1968)
- [9] Meyer R.B., *Appl. Phys. Lett.*, **12** 281 (1968)
- [10] Yamashita M., *J.Phys.Soc.Japan* **57** (1988) 2051
- [11] Yamashita M., *Prog.Theor.Phys* **74** (1985) 622

[12] Michelson **A.**, *Phys.Rev.Lett* 39 (1977) 464

[13] Yamashita M., *J.Phys.Soc.Japan* 56 (1987) 1414